Multifunctional dendronized polypeptides for controlled adjuvanticity

Zhiyuan Fan,[†] Sharon Jan,[‡] James C. Hickey,[†] D. Huw Davies,[‡] Jiin Felgner,[‡] Philip L. Felgner,[‡], and Zhibin Guan[†], [#], §, ^,*

* Corresponding author:

Department of Chemistry, University of California, Irvine, CA 92697, USA Email: zguan@uci.edu

Department of Physiology and Biophysics, School of Medicine, University of California, Irvine, CA 92697, USA

Email: pfelgner@uci.edu

[†] Department of Chemistry, University of California, Irvine, CA 92697, USA

[‡] Department of Physiology and Biophysics, School of Medicine, University of California, Irvine, CA 92697, USA

Department of Biomedical Engineering, University of California, Irvine, CA 92697, USA

[§] Department of Chemical and Biomolecular Engineering, University of California, Irvine, CA 92697, USA

[^] Department of Materials Science and Engineering, University of California, Irvine, CA 92697, USA

ABSTRACT

Vaccination has been playing an important role in treating both infectious and cancerous diseases. Nevertheless, many diseases still lack proper vaccines due to the difficulty to generate sufficient amounts of antigen-specific antibodies or T cells. Adjuvants provide an important route to improve and direct immune responses. However, there are few adjuvants approved clinically and many of them lack the clear structure/adjuvanticity relationship. Here we synthesized and evaluated a series of dendronized polypeptides (denpols) functionalized with varying tryptophan/histidine (W/H) molar ratios of 0/100, 25/75, 50/50, 75/25, and 100/0 as tunable synthetic adjuvants. The denpols showed structure-dependent inflammasome activation in THP-1 monocytic cells and structurerelated activation and antigen cross-presentation in vitro in bone marrow-derived dendritic cells. We used the denpols with bacterial pathogen Coxiella burnetii antigens in vivo, which showed both high and tunable adjuvating activities, as demonstrated by the antigen-specific antibody and T cell responses. The denpols are easy to make and scalable, biodegradable, and highly adjustable chemical structures. Taken together, denpols show great potential as a new and versatile adjuvant platform that allows us to adjust adjuvanticity based on structure-activity correlation with the aim to fine-tune the immune response, thus advancing vaccine development.

1. Introduction

Vaccination is a very successful strategy for combating both infectious and cancerous diseases ^{1,2}. Timely, COVID-19 vaccines are playing a pivotal role in helping stop the COVID-19 pandemic worldwide 3, 4. Clinical studies have shown that COVID-19 mRNA vaccination generates significantly higher amounts of antibodies than natural infections ^{5,6}. Vaccines have also been successfully developed to prevent many other infectious diseases clinically ⁷ and treat cancers preclinically 8,9. Nevertheless, vaccines are unavailable for many intracellular pathogen-associated diseases due to the difficulty to generate sufficient amounts of antigen-specific antibodies or T cells ^{10,11}. Given that antigens and adjuvants are the two major components of most subunit vaccine formulations, various strategies have been investigated for optimizing each of these two components with the aim to improve the efficacy of vaccines. From the antigen perspective, researchers have made great progress by using more immunogenic antigens such as proteins with altered structures or neoantigens ^{12,13}. mRNA vaccines are a revolutionary new strategy for which mRNAs are translated into target antigens in our bodies, as in the case of the highly efficacious COVID-19 vaccines developed by Moderna and Pfizer-BioNTech companies, respectively ^{3, 14}. Complementary to new antigen developments, adjuvants provide another route to enhance immune responses 15. However, there are relatively few adjuvants available and many of them lack molecular details and tunability 15.

An adjuvant is a substance that increases and/or modulates the immune response to a vaccine. Adjuvants enhance the activation of antigen-presenting cells (APCs) and the generation of antigen-specific T cells through several different mechanisms including Toll-like receptor (TLR) activation, inflammasome activation, stimulator of interferon genes (STING) pathway activation, or simply a depot effect ¹⁶. These may include Th1 responses associated with opsonizing antibodies

and cytotoxic T cells against intracellular pathogens or Th2 responses with neutralizing antibodies against extracellular pathogens ^{17,18}. Natural adjuvants such as ssRNA/dsRNA, lipopolysaccharide (LPS), and DNA have been studied for more than 100 years ¹⁹. The adjuvanticity of aluminum-based salts (e.g., aluminum hydroxide or aluminum phosphate) was discovered in the 1930s and they have been widely used in many vaccines, despite the unclear mechanism of their adjuvanticity ^{20,21}. In the 1990s and 2000s, oil-in-water emulsion-based adjuvants such as MF59 and AS03 have been developed for influenza vaccines ^{22,23}. Furthermore, combining the effect of TLR agonist and aluminum salts, AS04 consisting of 3-O-desacyl-4'-monophosphoryl lipid A (MPLA) and aluminum hydroxide was shown to increase adaptive immunity and was approved for human papillomavirus (HPV) vaccines in 2009 ²⁴. More recently, CpG oligodeoxynucleotides (CpG ODN) were approved in a hepatitis B vaccine in 2017, which interacts with TLR9 to exert its adjuvanticity

Several other natural or synthetic adjuvants have also been investigated, such as saponin-based adjuvants ^{26, 27}, zwitterionic polysaccharides ²⁸, and α-galactosylceramide derivatives ²⁹. AS01 containing MPLA and saponin QS-21 can help generate durable immune responses and have been approved for the shingles vaccine ³⁰. Synthetic polymers have shown adjuvanticity via the depot effect ³¹. Interestingly, nanoparticles made from an ultra-pH-sensitive polymer can activate the STING pathway to generate a robust Th1 response ³² and polyethyleneimines grafted with fluoroalkane can interact with antigens to form nanoparticles and stimulate immune cells via TLR4 ³³. Meanwhile, significant efforts have been made to reformulate the classic adjuvants such as conjugating hydrophobic tails to CpG ODN ³⁴ and changing the morphology/nanostructure for aluminum salts ³⁵. Despite more than a century of research, the repertoire of vaccine adjuvants used clinically is still very limited. In addition, many adjuvants are complex in structure (e.g., QS-

21), hard to synthesize in a cost-effective manner, and lack tunability. For further vaccine development, there is an urgent need for new synthetic adjuvants that have well-defined chemical structures, are easy to make at scale, and have tunable adjuvanticity. Such new adjuvants should improve the efficacy of vaccines and broaden vaccine prevention of many diseases. Furthermore, tunable adjuvants would provide a platform for rationally designed adjuvants based on structure-activity correlation, allowing us to modulate the immuno-stimulation to maintain safety.

We have previously developed a series of multifunctional dendronized polypeptides (denpols) initially for siRNA and mRNA delivery ^{36,37}. In a recent study, we showed that some of the denpols carrying certain amounts of histidine (H) and tryptophan (W) residues could enlarge and rupture endolysosomes to activate the NLR family pyrin domain containing 3 (NLRP3) inflammasome pathways ³⁸. As inflammasome activation is one major pathway for immunestimulation, we hypothesized that functionalized denpols could serve as adjuvants for vaccine purposes. The denpols have several advantages to offer as synthetic adjuvants: 1) they are easy to make and scalable; 2) they are composed entirely of amino acid building blocks and are thus fully biodegradable; and 3) importantly, they are highly tunable in chemical structure which can be exploited to adjust adjuvanticity based on structure-activity correlations. Furthermore, our previous studies have shown that the functionalization of the tryptophan (W) residue on denpols facilitates their cell uptake, while the functionalization of the pH-responsive histidine (H) residue enhances their endosomal rupture capabilities ^{36, 37}. To systematically investigate the adjuvant effects of the denpol system, in this study we synthesized a series of generation-three (G3) denpols functionalized with varying W/H molar ratios of 0/100, 25/75, 50/50, 75/25, and 100/0. Our in vitro studies of this series of denpols showed structure-dependent inflammasome activation in THP-1 cells and controlled BMDC activation and antigen cross-presentation. Encouraged by the

in vitro activities, we tested the denpols as adjuvants in vaccine formulations with Coxiella burnetii antigens in vivo. The denpols showed both high and tunable adjuvant activities, as demonstrated by the antibody generation and antigen-specific T cell responses.

2. Materials & methods

2.1. The synthesis and characterization of G3 Denpols

Generation-three (G3) denpol was synthesized as previously reported ^{36,37}. The free amino groups on the periphery of each dendron provide convenient handle for further conjugation of H and W residues. To synthesize G3 denpol functioned with 0%W and 100%H (G3 0%W), 25%W and 75%H (G3 25%W), 50%W and 50%H (G3 50%W), 75%W and 25%H (G3 75%W), and 100%W and 0%H (G3 0%W), G3 denpol (30 mg, 1 equiv defined as one repeat unit) was dissolved in 3 mL of N,N-dimethylformamide (DMF, Fisher Scientific) into which benzotriazol-1yloxytripyrrolidinophosphonium hexafluorophosphate (PyBOP, Oakwood Chemical) (93.69 mg, 24 equiv) and N,N-diisopropylethylamine (DIPEA, Fisher Scientific) (23.29 mg, 24 equiv) were added. The calculated amounts of Boc-His(Boc)-OH.DCHA (Aapptec) and Boc-Trp(Boc)-OH (Chem-Impex) (the total amounts were 24 equiv) were added to functionalize denpols for 24 h under stirring. The next day, the reaction solutions were transferred to dialysis tubings with MWCO 3.5 kD (Spectrum Chemical) and the tubings were immersed in 1 L of methanol (Fisher Scientific). The dialysis went on for 24 h and methanol was changed every 6 h for the first 12 h. The solutions were then transferred to scintillation vials (Fisher Scientific) and the solvents were then removed by rotary evaporation. To remove all protecting groups on the functionalized denpols, trifluoroacetic acid (4 mL, Fisher Scientific), dichloromethane (1 mL, Fisher Scientific), and triisopropyl silane (0.1 mL, Fisher Scientific) were then added to the vials and the solutions were

stirred at r.t. for 4 h. Solvents were then removed by rotary evaporation and methanol (10 mL) was added to dissolve the polymers. The dissolved denpols were dialyzed against methanol in dialysis tubings with MWCO 3.5 kD for 24 h. Methanol was changed every 6 h for the first 12 h. The solutions were then transferred to scintillation vials, with the solvents being removed by rotary evaporation and the polymers dried under high vacuum overnight to yield yellow films in the vials. The yields were around 75%. G3 denpols were dissolved in D_2O and their 1H NMR spectra were characterized by a 600 MHz Bruker instrument. As shown in Figure S4, the integration between 8.0 and 8.8 ppm represents hydrogen a from H, thus indicating the relative amount of H. The integration between 6.7 and 7.7 ppm represents hydrogen b from H and five hydrogen c from W. Therefore, the W/H ratios were calculated from those two integrations and the actual ratios are 0%W (G3 0%W), 26%W (G3 25%W), 51%W (G3 50%W), 75%W (G3 75%W), and 100%W (G3 100%W).

To sterilize the polymers, all G3 denpols were dissolved in water, filtered through 0.45µm syringe filters (VWR), and lyophilized and stored in -80 °C before use.

2.3. Characterization of G3 denpols

To study the sizes and zeta potentials of G3 denpols, polymers were dissolved in water at 1 mg/mL concentration. Dynamic light scattering (DLS) was used to measure the sizes of denpols in disposable cuvettes (Fisher Scientific) at 25 °C on a Zetasizer Nano ZS (Malvern). Zeta potentials were measured using the same instrument at 25 °C. For transmission electron cryomicroscopy (cryoTEM), sample vitrification was performed with a Leica EMGP plunger (Leica microsystem Inc, Buffalo Grove IL). Briefly, 3 ul of G3 75%W (2 mg/mL in water) was applied to glow discharged Quantifoil grids (R1.2/1.3, Electron Microscopy Sciences, Hatfield

PA). The grid was quickly plunged into liquid propane after 3.5s blotting at 95% humidity. The frozen hydrated specimen was then transferred onto a Gatan-915 cryo-transfer holder (Gatan/Ametec, Pleasation CA) and examined under a JEM-2100F electron microscope (JEOL USA, Peabody MA) with operation voltage at 200kV. The images were recorded at electron dose less than 15 e/A² and collected on a Gatan OneView CCD at a magnification of 30,000x, which corresponding respectively to 3.1 Angstrom per pixel at specimen space.

2.4. THP-1 cell inflammasome activation study

THP-1 cell cultured in RMPI 1640 complete medium (Gibco) with 10% of fetal bovine serum (FBS, Corning) and 50 μM of beta-mercaptoethanol (Sigma) were plated into a 96-well flat-bottom tissue culture plate (VWR) and LPS (Sigma Cat # L2630) was added to prime cells with a final concentration of 10 ng/mL. After 3 h, supernatants were slowly removed by pipetting and fresh media was added. Samples including adenosine triphosphate (ATP, Thermo Scientific Cat# R0441) (0.625 mM), alum (suspension of aluminum hydroxide and magnesium hydroxide, Imject Alum, Thermo Scientific) (50, 100, and 200 μg/mL) and denpols (50, 100, and 200 μg/mL) were added to stimulate the secretion of IL-1β from THP-1 cells. After 24 h, HEK-Blue IL-1β cells cultured in DMEM complete media (10%_of FBS and 1% of penicillin-streptomycin (PS)) were plated into a 96-well flat-bottom tissue culture plate, into which 50 μL of supernatants of the denpol-treated THP-1 cells were added. Known concentrations of human IL-1β protein (BioLegend) (160, 80, and 40 pg/mL) were used as positive controls. After overnight culture, 20 μL of supernatants of HEK-Blue IL-1β cells were transferred to a 96-well flat-bottom tissue culture plate with 180 μL of QUANTI-BLUE Solution (InvivoGen, San Diego Cat# rep-qbs) in

each well. The absorption at 620 nm was recorded using a Multiskan[™] FC microplate photometer and the IL-1β activities were normalized based on the reading of IL-1β control (160 pg/mL).

2.5. BMDC culture and activation study

Bone marrow was flushed out from the hind leg bones of a female C57BL/6 mouse (Charles River) with RPMI 1640 medium on day 0. Bone marrow cells were dispersed by pipetting and filtered through a 70-μm nylon strainer (VWR). Cells were spun down at 300 x g for 5 mins and red blood cells were lysed by resuspending the pellets in 2 mL of RBC lysis buffer (Tonbo Bioscience) for 5 mins. Ten mL of RMPI 1640 complete medium (10% of FBS, 1% of PS, and 50 μM of beta-mercaptoethanol) was added and the cells were spun down at 300 x g for 5 mins. The cell pellet was dispersed with RMPI 1640 complete medium and cells were culture in Petri dishes (Falcon) at 0.5 million per mL with 20 ng/mL of granulocyte-macrophage colony-stimulating factor (GMCSF, BioLegend) at 37 °C in an incubator supplied with 5% CO₂. On day 3 and day 5, cells were spun down and replaced with fresh media with 20 ng/mL of GM-CSF. On day 6, cells were detached by using phosphate-buffered saline (PBS, Gibco) with 3 mM of ethylenediaminetetraacetic acid (EDTA, Fisher Scientific) and replated into 96-well flat-bottom non-treated plates (Corning) for various experiments.

BMDCs were treated with LPS (1 μg/mL), MPLA (Avanti Polar Lipids, 1 μg/mL), CpG ODN 1018 (CpG, IDT) (1 μg/mL), alum (50, 100, and 200 μg/mL), or denpols (50, 100, and 200 μg/mL) for 24 h at 37 °C in an incubator supplied with 5% CO₂. Cells were detached by using PBS with 3 mM of EDTA and spun down at 300 x g for 5 mins. Cells were first incubated with anti-CD16/32 (BioLegend) and then stained with propidium iodide (PI, Invitrogen), PE anti-mouse CD11c antibody (BioLegend), APC/Cyanine7 anti-mouse CD86 antibody (BioLegend), APC anti-

mouse CD80 antibody (BioLegend), Pacific Blue[™] anti-mouse CD40 antibody (BioLegend), and PerCP anti-mouse I-A/I-E antibody (BioLegend) for 30 mins at room temperature. Cells were washed twice with PBS with 4% of FBS (FACS buffer), resuspended in FACS buffer with 1% of paraformaldehyde (PFA, Alfa Aesar). The cells were characterized on a BD LSRFortessa flow cytometer and the data were analyzed by using FlowJo (Tree Star).

2.6. Antigen cross-presentation study

Ovalbumin (OVA) peptide SIINFEKL (Sigma) (0.5 µg/mL) or OVA whole proteins (Sigma) (500 µg/mL) were added to BMDCs cultured in 96-well flat-bottom non-treated plates in RPMI 1640 complete medium. Then LPS (1 µg/mL), MPLA (1 µg/mL), CpG (1 µg/mL), alum (50, 100, and 200 µg/mL), or denpols (50, 100, and 200 µg/mL) were added to certain wells and the cells were kept at 37 °C in an incubator supplied with 5% CO₂ for 24 h. Cells were detached by using PBS with 3 mM of EDTA and spun down at 300 x g for 5 mins. Cells were first incubated with anti-CD16/32 and then stained with APC anti-mouse CD11c antibody (BioLegend) and PE anti-mouse H-2Kb bound to SIINFEKL antibody (Biolegend) for 30 mins at room temperature. Cells were washed twice with FACS buffer, resuspended in FACS buffer with 1% of PFA. The cells were characterized on a BD LSRFortessa flow cytometer and the data were analyzed by using FlowJo.

2.7. Cell uptake and mechanism study

Each of the denpols (5 mg), including G3 0%W, G3 25%W, G3 50%W, and G3 75%W, was dissolved in DMF containing DIPEA (1 mg), and 16.6 μg of Alexa Fluor 647 NHS Ester (Succinimidyl Ester) (Invitrogen) dissolved in dimethyl sulfoxide (Fisher Scientific) was added.

The reaction solutions were stirred for 24 h at room temperature and were put into dialysis tubings with MWCO 3.5 kD immersed in methanol for 24 h. Methanol was changed every 6 h for the first 12 h. The solutions were then transferred to scintillation vials and were removed by rotary evaporation and the polymers were under high vacuum overnight to yield Alexa Fluor 647-modified denpols (AF647-denpols). The yield was around 80%. AF647-denpols were dissolved in water and filtered before use for cell uptake experiments.

For the uptake experiment, the fluorescence intensities of AF647-denpols at 670 nm were adjusted by using a Tecan Spark plate reader with an excitation at 640 nm. BMDCs were cultured in 96-well flat-bottom non-treated plates in RPMI complete medium, and either PBS or AF647-denpols (200 µg/mL) were added to treat BMDCs for 24 h at 37 °C in an incubator supplied with 5% CO₂. Cells were detached by using PBS with 3 mM of EDTA and spun down at 300 x g for 5 mins. Cells were first incubated with anti-CD16/32 and then stained with PE anti-mouse CD11c antibody for 30 mins at room temperature. Cells were washed twice with FACS buffer, resuspended in FACS buffer with 1% of PFA. The cells were characterized on a BD LSRFortessa flow cytometer and the data were analyzed by using FlowJo.

For the confocal experiments, BMDCs were cultured on confocal dishes (VWR) with 0.3 million cells in each dish. The next day, either PBS or AF647-denpols (200 µg/mL) were added to treat BMDCs for 24 h at 37 °C in an incubator supplied with 5% CO₂. Cells were washed with PBS twice and Hoechst (Thermo Scientific) was used to stain some of the cells for 30 min at room temperature. Some cells were stained with 200 µL of Magic Red staining (Immunochemistry Technologies, MN) for 30 mins at room temperature first and then stained with Hoechst for 30 min at room temperature. Cells were washed with PBS twice and imaged using a Zeiss LSM700 confocal microscope.

2.8. In vivo immunization study

Female C57BL/6 mice (7-9 week old, Charles River) were used for the in vivo vaccine study. All procedures were carried out by following protocols approved by UC Irvine's Institutional Animal Care and Use Committee. C. burnetii antigen CBU1910 was used as previously reported ³⁹. We had 5 experimental groups with the following formulations: PBS control, CBU_1910 only $(3.3 \mu g)$, alum $(1 mg) + CBU_1910 (3.3 \mu g)$, $G3 25\% (1 mg) + CBU_1910 (3.3 \mu g)$ μ g), G3 50% (1 mg) + CBU_1910 (3.3 μ g), and G3 50% (1 mg) + CBU_1910 (3.3 μ g). Mice were randomly assigned into groups and each group had 5 mice. For immunization, 50 µL of each formulation was injected intramuscularly into the right thigh on day 0. On day 14, 50 µL of each formulation was injected intramuscularly into the right hind leg again as the boost. The weights of each mouse were monitored frequently until day 28. On day 28, blood was collected from the submandibular vein into Eppendorf tubes and mice were sacrificed. Spleens were collected and stored in cold PBS. The spleens were homogenized with plungers from 3-mL syringes (BD) and were incubated in cell dissociation buffer (Gibco) with liberase (Sigma) and DNase I (Thermo Scientific) for 15 min at room temperature. Then the solution was drained through a 70-µm strainer (Fisher), which was rinsed with 10 mL of FACS buffer. The solution was centrifuged at 400 x g for 5 mins and the supernatant was discarded. The pellet was resuspended in 2 mL of RBC lysis buffer and incubated at room temperature for 8 mins. FACS buffer was added and the solution was centrifuged at 400 x g for 5 mins. The pellet was resuspended in RPMI 1640 complete medium and the cell number was counted by using a hemocytometer.

2.9. Quantification of CBU_1910 antibodies

Blood collected in tubes from the *in vivo* studies was centrifuged at 800 x g for 5 min to collect the serum. The CBU_1910 antibodies were quantified by using a protein microarray method as reported ³⁹. Serum samples were diluted in blocking buffer (GVS, Sanford, ME) with *E. coli* lysate (Genescript), which were added on microarray slides and incubated at 4 °C overnight. The slides were washed 6 times with Tris-buffered saline with 0.05% Tween 20 (TBST) and secondary antibodies diluted 1:200 including biotin-SP (long spacer) AffiniPure Goat Anti-Mouse IgG (Jackson ImmunoResearch Laboratories, PA), biotin-SP (long spacer) AffiniPure Goat Anti-Mouse IgG1 (Jackson ImmunoResearch Laboratories, PA), and biotin-SP (long spacer) AffiniPure Goat Anti-Mouse IgG2c (Jackson ImmunoResearch Laboratories, PA) were added to the slides and the slides were shaken at room temperature for 1 h. Then the slides were washed with TBST 6 times and QdotTM 800 Streptavidin Conjugate (Thermo Scientific) diluted 1:250 was added to the slides and the slides were shaken at room temperature for 1 h. The slides were then washed 3 times with TBST, rinsed in water, and air-dried. The slides were imaged on an ArrayCAM Imaging System (Grace Bio-Labs) and the antibody fluorescence intensities were processed.

2.10. Antigen-specificity study of T cells

For antigen-specific T cell cytokine study, 1 million splenocytes in 0.1 mL of RPMI 1640 complete medium (10% of FBS, 1% of PS, and 50 μ M of beta-mercaptoethanol) were culture either with CBU_1910 (10 μ g/mL) or OVA (10 μ g/mL) in 96-well round-bottom tissue culture plates (VWR) at 37 °C in an incubator supplied with 5% CO₂ for 16 hours. The plate was centrifuged at 400 x g for 5 mins and supernatants were collected. The cytokine concentrations were quantified using a LEGENDplex assay (BioLegend 741043) according to the manufacturer's instructions.

For antigen-specific CD8+ T cell study, BMDCs were cultured with CBU_1910 (10 µg/mL) or OVA (10 µg/mL) in 96-well U-bottom tissue culture plates (VWR) in complete medium (0.1 million in 100 µL per well) overnight. The next day, the plate was spun at 300 x g for 5 min and the supernatants were removed. Splenocytes (1 million/well) and human IL-2 (5 ng/mL, BioLegend) were added to the wells and cultured at 37 °C in an incubator supplied with 5% CO₂. After 1 h, brefeldin/monensin (1x, BioLegend) were added 1 h and the cells were cultured for another 4 h in the incubator. Cells were spun down at 300 x g for 5 mins and washed with PBS. Cells were first incubated with anti-CD16/32 and then stained with APC/Cyanine7 anti-mouse CD3 antibody (BioLegend), AF700 anti-mouse CD4 antibody (BioLegend), FITC anti-mouse CD8a antibody (BioLegend), and propidium iodide (BioLegend). Cells were then intracellularly stained with PE anti-mouse IFN-γ antibody (BioLegend) and BV421 anti-mouse TNF-α antibody (BioLegend). The cells were characterized on a BD LSRFortessa flow cytometer and the data were analyzed by using FlowJo.

2.10. Statistical analysis

Data were presented as mean \pm standard deviation (SD) or mean \pm standard error of the mean (SEM) as specified in the corresponding figure captions. For the statistical significance analysis of multiple groups, one-way ANOVA was used for the calculations, followed by Tukey's multiple comparison test.

3. Results and discussion

3.1. Synthesis and characterization of G3 denpols

The G3 denpols used in this study were synthesized by following our previously reported methods ^{36, 37}. In brief, we first prepared the backbone polymer by step-growth polymerization of dicysteine and L-lysine. Next, onto each repeat unit of the linear polymer backbone we grew G3 lysine dendrons composed of three layers of L-lysine via peptide coupling reactions to generate the basic G3 denpol architecture. Finally, we functionalized the lysine dendrons on the G3 denpol by conjugating various amounts of H and W at the periphery of dendrons via peptide coupling reactions. For the structure-activity correlation study, we prepared a series of multifunctional G3 denpols carrying the following molar ratio of W/H: 0/100, 25/75, 50/50, 75/25, and 100/0, respectively. The molecular architecture of the G3 denpols is schematically shown in Figure 1A (full chemical structures and the synthetic route of G3 50%W shown in Figure S1). The chemical structure and compositions of the series of G3 denpols were confirmed by ¹H NMR spectra (Figure S2-S6). For simplicity, in later discussion the denpols will be referred to by their mol% of W in the periphery functionalities. For example, a G3 denpol with 25/75 W/H periphery functionalization will be called G3 25%W. It should be noted that the entire synthesis process was conducted under mild conditions with simple peptide coupling at room temperature. The G3 denpols are fully biodegradable as the disulfide bonds in the polymer backbone can break down in cells by reduction and all the peptidyl linkages in the polymer constructs can be degraded by proteases as shown in our previous studies 40. The full biodegradability ensures safety for the denpols as shown in our in vivo vaccination studies (vide infra).

After synthesizing the G3 denpols, we characterized their biophysical properties in aqueous solution using Dynamic Light Scattering (DLS). As shown in Figure 1B, most denpols showed bimodality in DLS size distribution, with one peak at smaller sizes (18 - 28 nm) and another peak at larger sizes (>140 nm), suggesting the co-existence of monomeric G3 denpols and their self-

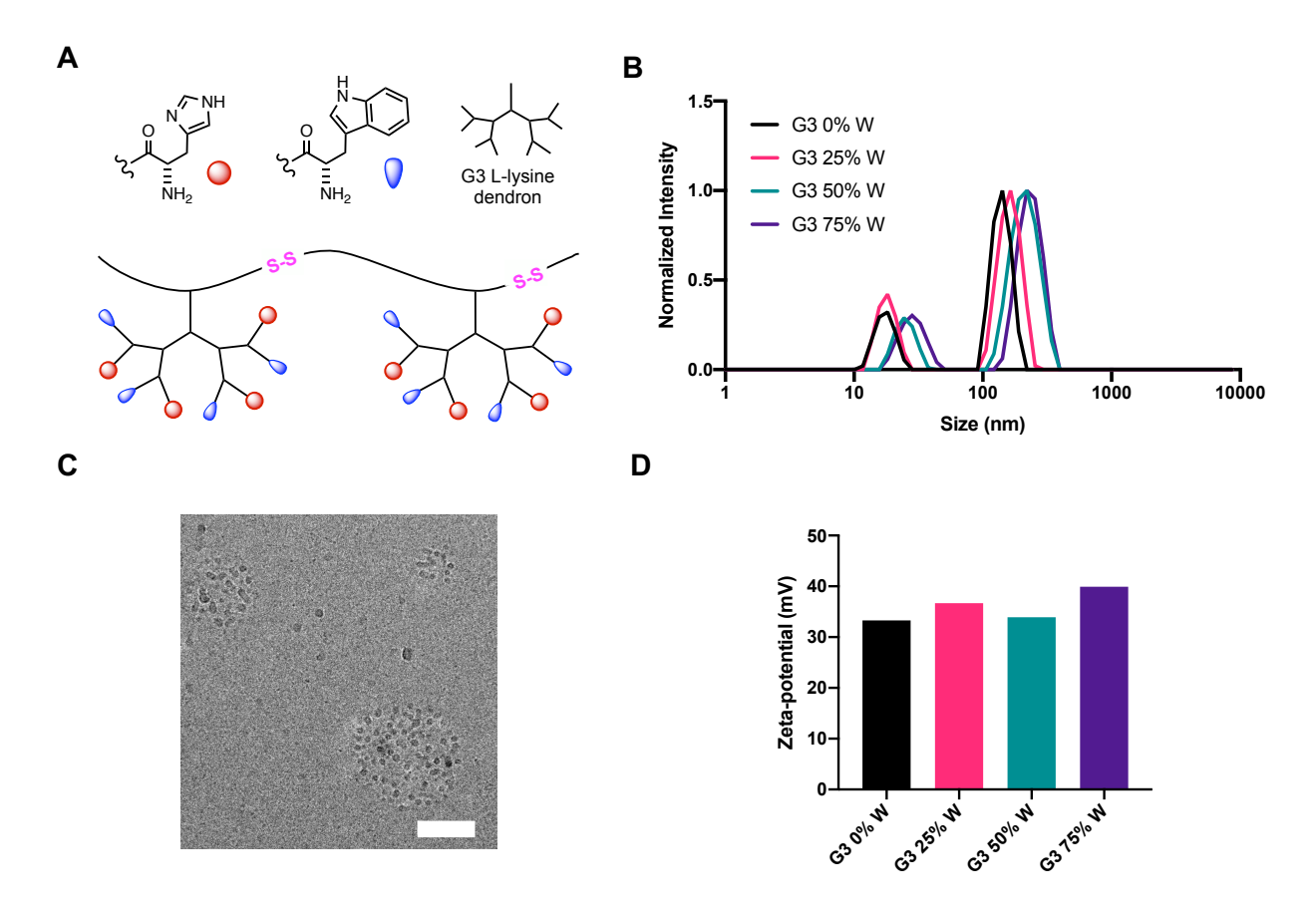


Figure 1. Synthesis and characterizations of G3 denpols. A) An illustration of G3 denpols. G3 0%W, G3 25%W, G3 50%W, and G3 75%W were prepared by functionalizing G3 denpol with various ratios of H and W. B) The size distributions of G3 denpols in water measured by DLS. C) A representative cryoTEM image of G3 75%W. Scale bar, 100 nm. D) The zeta-potentials of G3 denpols in water.

assembled nanoparticles in aqueous solution which is in agreement with the cryoTEM image of G3 75%W (Figure 1C). Both peak sizes increased with the percentage of W in G3 denpols due to the hydrophobicity of W. Having a large amount of W, G3 100%W was unstable and had large aggregates in water (data not shown). Therefore, G3 100%W was not included in the following *in vitro* and *in vivo* studies. All G3 denpols were positively charged with zeta-potentials around +35 mV (Figure 1D), because of the α-amine groups on H and W residues.

3.2 Inflammasome activation by denpols in THP-1 cells

THP-1 cells have been widely used as a standard cell line for inflammasome activation 41. Therefore, we employed them to study the inflammasome activities of denpols. Our recent study has confirmed the activation of the inflammasome pathways by denpols via IL-1β secretion, apoptosis-associated speck-like protein containing a caspase recruitment domain staining, and caspase-1 staining ³⁸. Hence, we monitored the inflammasome activities via the IL-1β secretion, which was indirectly quantified by using HEK-BLUE IL-1β cells and the QUANTI-BLUE assay. Negative controls showed that THP-1 cells had low IL-1β secretion by themselves or after being primed by LPS alone for 3 h (Figure 2A). While LPS priming activates the nuclear factor-κB (NF- κ B) pathway to generate pro-IL-1β, an NLRP3 inflammasome inducer is needed for the secretion of mature IL-1\beta. As a positive control, ATP, a common inflammasome activator, increased the IL-1β secretion by 2 times. Alum, a widely used adjuvant in vaccines, increased the IL-1β activity by 30% at 200 μg/mL dosage compared with LPS alone, similar to previously reported results ³⁵, ⁴². In contrast, G3 denpols with relatively high W% showed high levels of inflammasome activation (Figure 2A). The IL-1β activities induced by denpols increased with the percentages of W and peaked around 50% W. Apparently, the level of W functionalization at the dendron periphery plays an important role in denpol's inflammasome activity, with the IL-1β activity for the 50% W denpol more than 5-fold higher than the 0% W denpol at 200 µg/mL dosage.

Next, we studied the dose-response relationship of denpols on inflammasome activation. All denpols exhibited dose dependence, with the denpols having higher levels of W showing more pronounced dose dependence. For 25%W, 50%W, and 75%W G3 denpols, 200 μ g/mL dose of samples generated much higher IL-1 β activities than doses at 50 μ g/mL and 100 μ g/mL (Figure 2B). However, alum did not show dose response at tested concentrations, which matched a

previous study showing low IL-1 β activities and no strong dose response of alum at 250 μ g/mL or lower ³⁵. In summary, we have shown that denpols could induce robust inflammasome activation in a dose-dependent manner and the activity peaked around 50%W for the denpols.

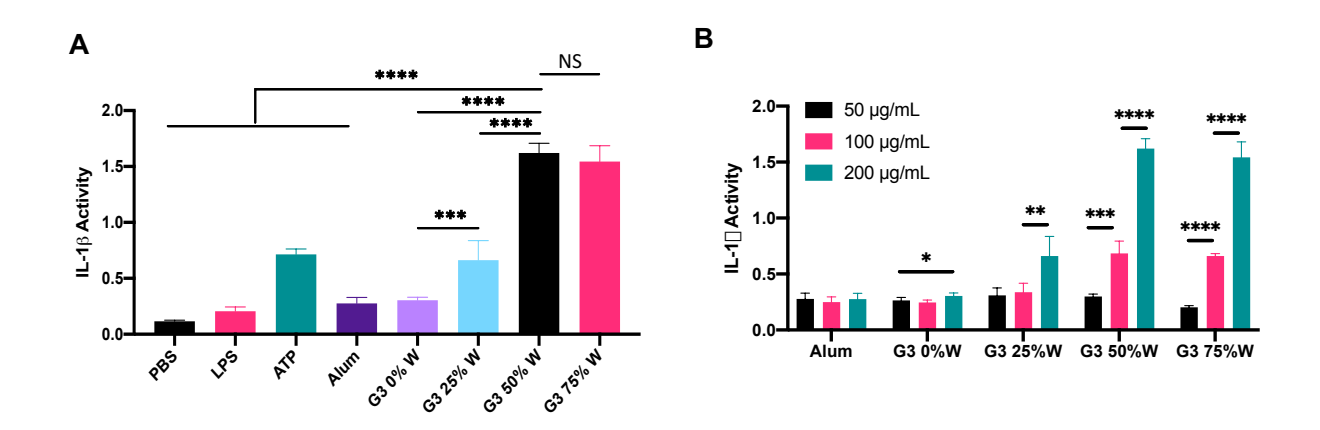


Figure 2. The inflammasome activation of THP-1 cells by denpols. A) The IL-1β activities of THP1 cells induced by ATP, alum, and denpols (0%W, 25%W, 50%W, and 75%W). THP-1 cells were primed with LPS (10 ng/mL) for 3 h and then were cultured with PBS, ATP (0.625 mM), alum (200 µg/mL), or denpols (200 µg/mL) for 24 h. B) The dose response of IL-1β secretion of THP-1 cells treated with 3 concentrations of denpols. THP-1 cells were primed with LPS (10 ng/mL) for 3 h and then were cultured with 50, 100, and 200 µg/mL of alum and denpols for 24 h. The induced IL-1β in the supernatants were quantified using HEK-BLUE IL-1β cells and the QUANTI-BLUE assay and were normalized using the reading of IL-1β (160 pg/mL). Values are plotted as mean \pm SD (n = 4). For the statistical significance analysis, one-way ANOVA was employed with Tukey multiple comparison test. NS: not significant, *p < 0.05, **p < 0.01, ****p < 0.001, ****p < 0.0001.

3.3 BMDC activation by denpols

After confirming the inflammasome activity of denpols using THP-1 cell assay, we used primary BMDCs (CD11c⁺) as standard APCs to evaluate the denpols' adjuvanticity *in vitro* by monitoring the stimulation of BMDC activation markers (Figure S7). Activation marker CD86 can bind to CD28 on T cells to activate them ⁴³. Common adjuvants such as LPS, CpG, MPLA, and alum have been shown to increase the CD86 expression in previous reports ^{35,44}. Encouragingly,

all denpols (200 µg/mL) caused increases in the mean fluorescence intensity (MFI) of CD86 with the MFI increasing with the percentages of W, which peaked around 50% of W (Figure 3A and Figure S8A). Notably, the CD86 MFI of BMDCs treated with G3 50%W was significantly higher than those treated with control adjuvants (1 µg/mL or 200 µg/mL for alum). Similar to the trend of inflammasome activity in THP-1 cell assay (Figure 2B), the concentration of denpols also had a significant impact on BMDC activation (Figure 3B). All denpols showed dose dependence and the denpols with G3 50%W and G3 75%W increased CD86 expression much more than alum at all concentrations.

Another activation marker CD40 can interact with CD40L on T cells to activate them ⁴⁵. Similar to the CD86 expression assays, at 200 μg/mL dosage denpols substantially increased the expression of CD40 with the increase level correlated with the percentages of W (Figure 3C and Figure S8B). The increase of CD40 expression peaked for G3 50%W, for which the CD40 MFI was significantly higher than the value for control adjuvants (1 μg/mL or 200 μg/mL for alum) and other denpols. Similarly, all denpols showed dose dependence for CD40 expression and the CD40 expression was much higher for G3 50%W and G3 75%W at 200 μg/mL than at 50 or 100 μg/mL (Figure 3D).

After BMDCs become activated, they upregulate the expression of MHC-II, which present peptides from exogenous antigens to prime CD4+ T cells. Therefore, MHC-II is an important activation marker for generating antigen-specific CD4+ T cells for the adaptive immunity ⁴⁶. Similar to the CD86 and CD40 results, the denpols (at 200 µg/mL) stimulated MHC-II expression to much higher levels than control adjuvants (1 µg/mL or 200 µg/mL for alum) and the expression increased with the percentages of W, which plateaued around 50% of W (Figure 3E and Figure S8C). Again, all denpols showed dose

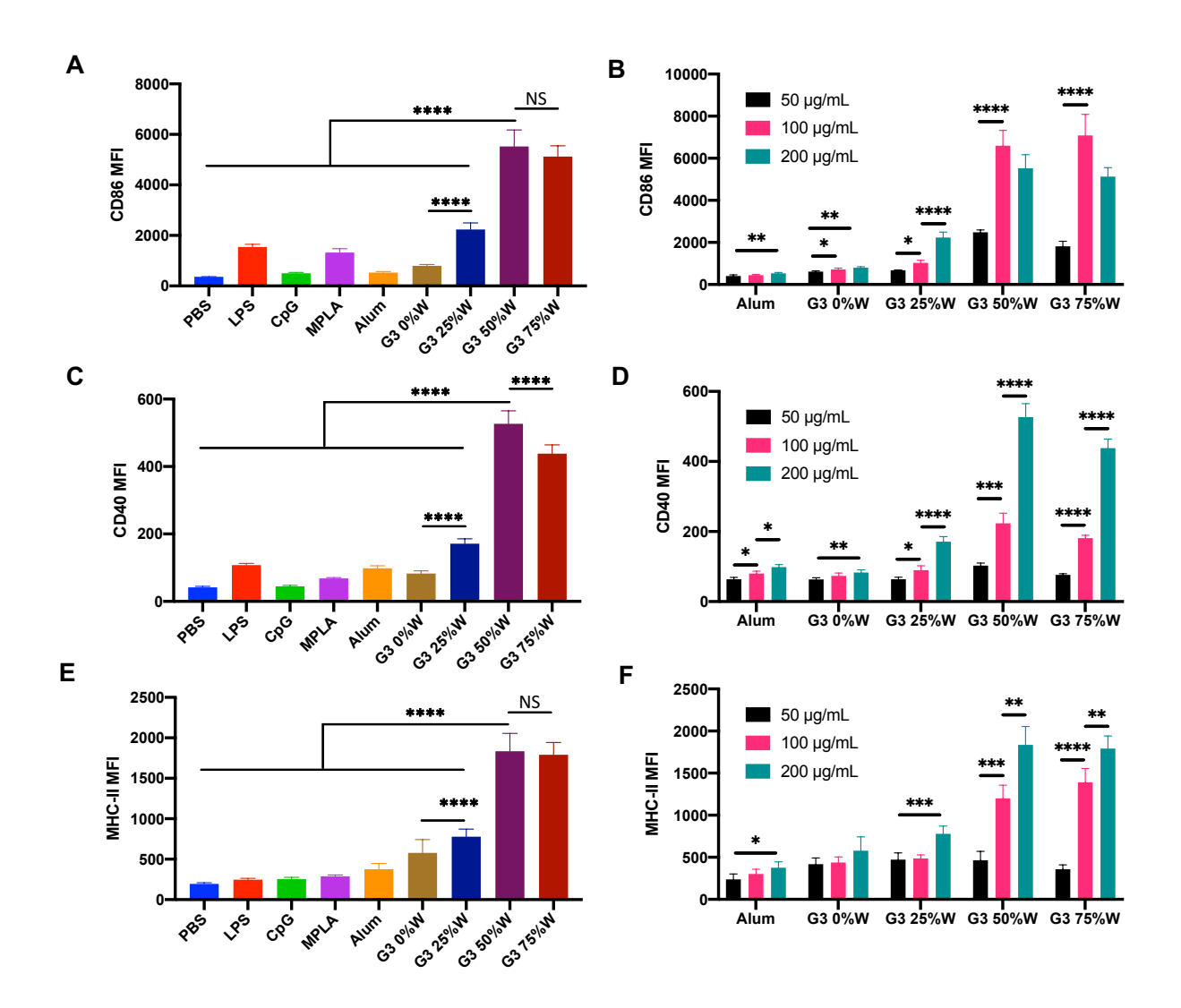


Figure 3. The adjuvanticity study of denpols using BMDCs *in vitro*. A) The CD86 MFIs of BMDCs treated with PBS, LPS (1 μg/mL), CpG (1 μg/mL), MPLA (1 μg/mL), alum (200 μg/mL), or denpols (200 μg/mL) for 24 h. B) The dose response of CD86 MFIs of BMDCs treated with alum or denpols at 50, 100, or 200 μg/mL. C) The CD40 MFIs of BMDCs treated with PBS, LPS (1 μg/mL), CpG (1 μg/mL), MPLA (1 μg/mL), alum (200 μg/mL), or denpols (200 μg/mL) for 24 h. D) The dose response of CD40 MFIs of BMDCs treated with alum or denpols at 50, 100, or 200 μg/mL. E) The MHC-II MFIs of BMDCs treated with PBS, LPS (1 μg/mL), CpG (1 μg/mL), MPLA (1 μg/mL), alum (200 μg/mL), and denpols (200 μg/mL) for 24 h. F) The dose response of MHC-II MFIs of BMDCs treated with alum or denpols at 50, 100, or 200 μg/mL. Values are plotted as mean \pm SD (n = 4). For the statistical significance analysis, one-way ANOVA was employed with Tukey multiple comparison test. NS: not significant, *p < 0.05, **p < 0.01, ****p < 0.001, ****p < 0.001, ****p < 0.001.

dependence for the MHC-II expression and the MHC-II expression was significantly higher for G3 50%W and G3 75%W at higher concentrations (Figure 3F).

We also studied the BMDC activation at a shorter time point (4 h). Denpols induced similar BMDC activation with lower MFIs for CD40 and MHC-II and also showed dose response (Figure S9). Overall, the BMDC activation marker results demonstrate that the denpols have high activity in stimulating BMDC activation markers including CD86, CD40, and MHC-II. The data also confirm that the adjuvanticity of denpols increases with their concentrations and the percentages of W, with the top performers being G3 50%W and G3 75%W.

3.4 Antigen cross-presentation of BMDCs induced by denpols

Antigen presentation plays critical roles in generating antigen-specific T cells by synergizing with activation marker/ligand interactions. Particularly, antigen cross-presentation in which exogenous antigens escape endosome/lysosome and are presented on MHC-I is a key step to generate antigen-specific CD8+ T cells. Studies have shown that antigen-specific CD8+ T cells are critical in preventing or ameliorating many diseases. Therefore, we also investigated whether denpols could improve the antigen cross-presentation.

We used both SIINFEKL short peptide and OVA whole protein as model antigens for the antigen cross-presentation study as both peptides and whole proteins have been used as antigens in vaccine formulations. Figure 4A shows that at 200 μ g/mL dosage denpols with 25% or higher of W boosted the SIINFEKL antigen cross-presentation significantly more than control adjuvants and the effect increased with the percentages of W (Figure 4A and Figure S10A). The MFI in the G3 50%W group was ~ 20 times higher than that in the SIINFEKL alone group, 4 times higher than those in the control adjuvant groups (1 μ g/mL or 200 μ g/mL for alum), and twice as high as

that in the G3 25%W group. G3 75%W was slightly better at promoting antigen cross-presentation than G3 50%W. Similarly, the concentration of denpols affected the antigen cross-presentation (Figure 4B). Alum and all denpols showed dose dependence. G3 50%W and G3 75%W at 50 ug/mL dose had significantly higher activities than alum at 200 µg/mL dose. Therefore, the denpols are highly effective in helping cross-present SIINFEKL on MHC-I of BMDCs.

However, there is some limitation with using the short peptide SIINFEKL for the cross-presentation study since the increased SIINFEKL-H-2K^b MFI can arise from the denpol-induced higher expression of MHC-I binding to free SIINFEKL in the solution without the process of internalization. Therefore, we further examined whether denpols could help BMDCs process whole OVA proteins and cross-present the antigen peptides. Even at a higher protein concentration (500 µg/mL), it was

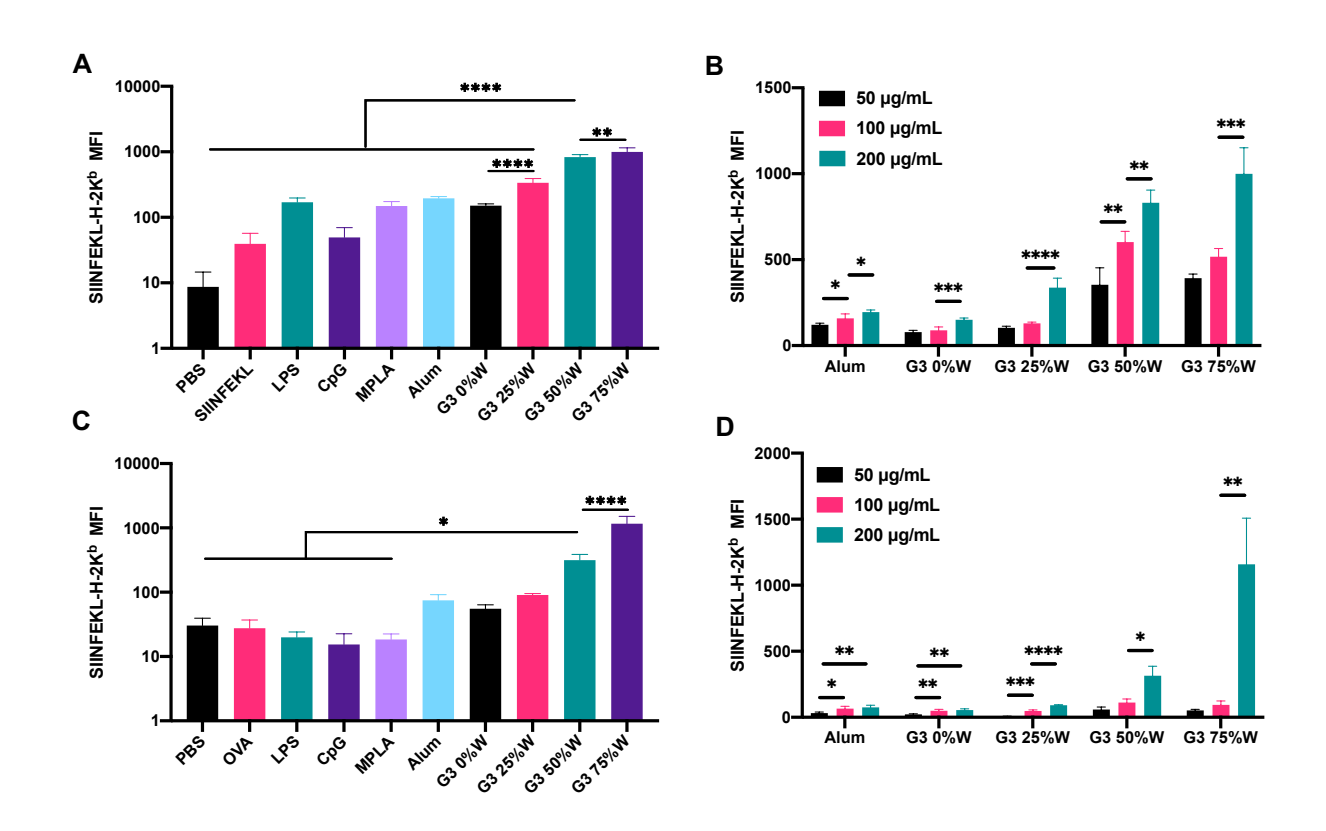


Figure 4. The antigen cross-presentation study of denpols using BMDCs in vitro. A) The SIINFEKL-H-2Kb MFIs of BMDCs pulsed with SIINFEKL (0.5 µg/mL) and treated with PBS, LPS (1 μg/mL), CpG (1 μg/mL), MPLA (1 μg/mL), alum (200 μg/mL), or denpols (200 μg/mL) for 24 h. B) The dose response of SIINFEKL-H-2Kb MFIs of BMDCs pulsed with SIINFEKL (0.5 μg/mL) and treated with alum or denpols at 50, 100, or 200 μg/mL. C) The SIINFEKL-H-2K^b MFIs of BMDCs pulsed with OVA (500 µg/mL) and treated with PBS, LPS (1 µg/mL), CpG (1 μg/mL), MPLA (1 μg/mL), alum (200 μg/mL), or denpols (200 μg/mL) for 24 h. D) The dose response of SIINFEKL-H-2K^b MFIs of BMDCs pulsed with OVA (500 µg/mL) and treated with alum or denpols at 50, 100, or 200 μ g/mL. Values are plotted as mean \pm SD (n = 4). For the statistical significance analysis, one-way ANOVA was employed with Tukey multiple comparison test. *p < 0.05, **p < 0.01, ***p < 0.001, ****p < 0.0001. much more difficult for BMDCs to process OVA protein and cross-present the antigen peptides (Figure 4C). Most of the control adjuvants, especially LPS, CpG, and MPLA (1 µg/mL) did not help much at all, with alum showing a slight increase of the MFI. In sharp contrast, G3 50%W and G3 75%W showed much more significant enhancement of the SIINFEKL presentation on MHC-I (Figure 4C and Figure S10B). G3 75%W showed ~ 10 times more enhancement than alum. The MFIs showed positive correlations with the concentrations of alum and denpols, with G3 50%W and G3 75%W showing dramatically increased MFI at the highest concentration (Figure 4D). Importantly, G3 50%W and 75%W not only help cross-present peptide antigens directly but also can process whole OVA proteins and cross-present the antigen peptides, which are highly desirable for adjuvant applications.

3.5 The uptake and distribution of denpols in BMDCs

As described in section 3.2-3.4, the *in vitro* cell culture studies of denpol adjuvanticity using both THP-1 cells and BMDCs showed an interesting correlation between the denpol structure and the adjuvant activities. Specifically, we observed a general trend of higher activities for denpols having higher ratios of W to H, with the maximum activities peaking at $\sim 50\%$ to 75% W. To gain an insight on which factors may contribute to such structure-activity correlation, we

conducted cell uptake and intracellular distribution studies of denpols in BMDCs. Previous studies have shown that because of its hydrophobicity and aromaticity, tryptophan can interact with cell membranes and bind to many membrane proteins, thus facilitating cell internalization ⁴⁷. Histidine has an imidazole ring (pKa ~6), which can capture protons at pH below 6. Therefore, the collection of histidine in acidic endolysosomes can cause osmotic swelling and disrupt the membrane, leading to vesicular escape ⁴⁸. Therefore, the percentages of H and W functionalization on denpols are expected to influence both their cell uptake efficiency and their capability to rupture endolysosomes after being internalized via endocytosis, both of which should influence the number of endolysosomes to be ruptured and the subsequent inflammasome activation level, thus impacting denpols' adjuvanticity.

For cell uptake and intracellular distribution studies, we conjugated denpols with AF647 fluorescence dye via the standard amine/NHS bioconjugation reaction. The uptake of denpols by BMDCs was quantified by flow cytometry. The cell uptake first increased with W percentage and then peaked at 50% W, with G3 50%W showing more than 5-fold cell uptake than G3 0%W and 2-fold more than G3 25%W (Figure 5A and 5B). The uptake of G3 75%W was slightly lower than that of G3 50%W. Next, we used confocal fluorescence microscopy to visualize the denpol distribution in cells. Similar to the results from flow cytometry, BMDCs internalized the smallest amount of G3 0%W and the largest amount of G3 50%W (Figure 5C), agreeing with our previous observation that W residues facilitate cell uptake ³⁶⁻³⁸. Furthermore, as shown in the AF647-Denpol channel and Higher magnification column, denpols also displayed different patterns in BMDCs. Denpols having relatively low W percentages (i.e., G3 0%W and G3 25%W) were distributed homogeneously in the cytoplasm, indicating that they could escape the endolysosomes easily due to their high percentages of histidine (H) residues that could facilitate endolysosome escape via

the so-called "proton sponge" effect ^{36,49}. In contrast, denpols having relatively high W percentages (i.e., G3 50%W and G3 75%W) show relatively large dots as well as strong fluorescence in the cytoplasm, suggesting that these denpols could enlarge and rupture endolysosomes. We also used Magic Red staining to detect the cathepsin B release from endolysosome rupture as described before ⁵⁰. The diffusion of cathepsin B fluorescence in the cytosol increased with the percentages of H in denpols and more punctate fluorescence was seen with higher percentages of W, which indicated the intact endolysosomes (Figure S11). Similarly, enlarged endolysosomes were observed in cells treated with G3 50%W and G3 75%W. Our observation matched the previously published results ³⁸ and confirmed that low uptakes of G3 0%W and 25%W limited their inflammasome activities. On the contrary, the combination of high cell uptakes of G3 50%W and 75%W and their sufficient capability to rupture endolysosomes resulted in strong inflammasome activation. Such combinatory effects of H and W help explain why G3 50%W and 75%W induced much stronger BMDC activation and antigen cross-presentation compared to other denpols.

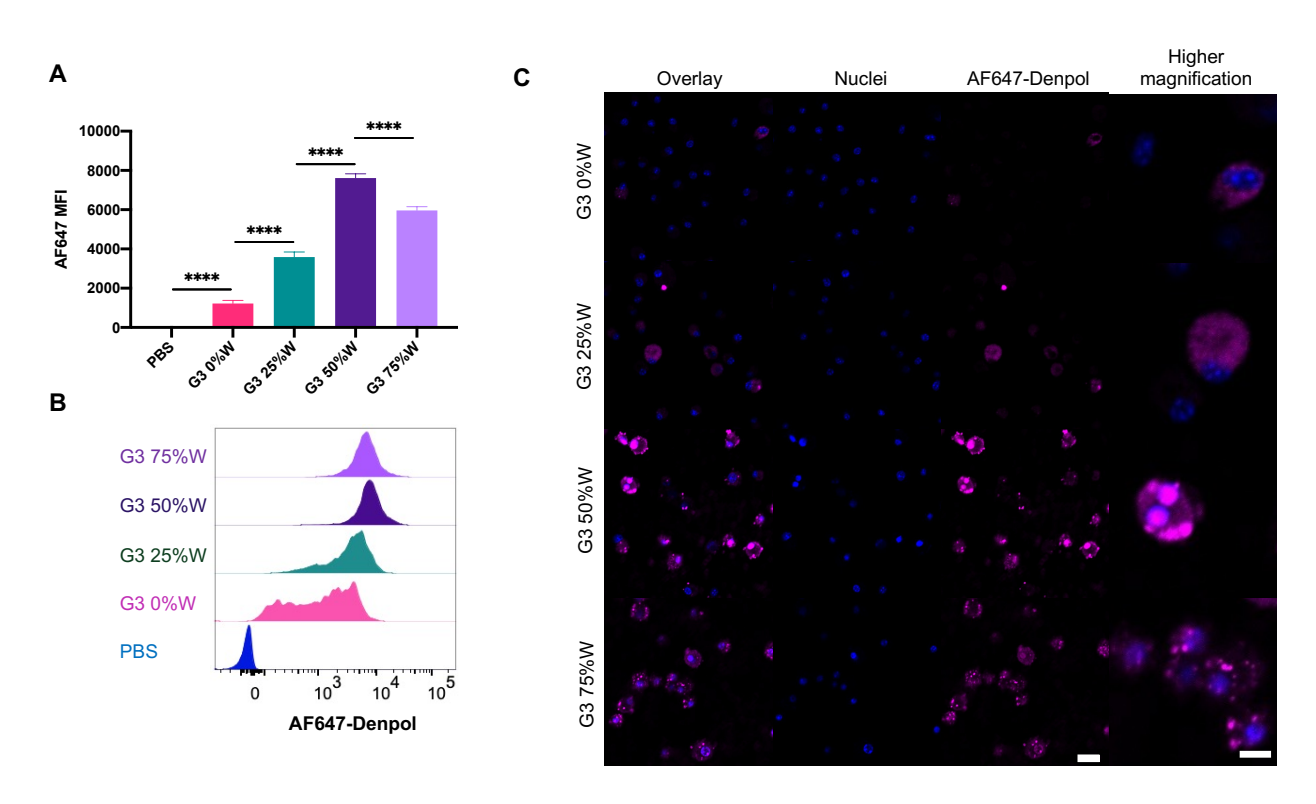


Figure 5. The study of denpol uptake by BMDCs using flow cytometry and confocal microscopy. A) The AF647-denpol MFIs of BMDCs treated with PBS or AF647-denpols (200 μg/mL) for 24 h. B) Representative histogram plots of AF647-denpol of BMDCs treated with PBS or AF647-denpols (200 μg/mL) for 24 h. C) The confocal images of BMDCs treated with AF647-denpols (200 μg/mL) for 24 h. The scale bar for Overlay, Nuclei, and AF647-Denpol is 20 μm and that for Higher magnification is 10 μm. Values are plotted as mean \pm SD (n = 4). For the statistical significance analysis of A, one-way ANOVA was employed with Dunnett multiple comparison test to G3 50%W. ****p <0.0001.

3.6 In vivo vaccine study

Given the strong performance of denpols on BMDC activation and antigen crosspresentation, we further evaluated their adjuvanticity in a Q fever vaccine. Q fever is a disease caused by the bacteria Coxiella burnetii. Currently, Coxiella burnetii bacteria are on the list of bioterrorism agents of the United States and there is no U.S. Food and Drug Administrationapproved vaccine available for this pathogen ^{39,51}. Based on the *in vitro* result, we selected G3 25%W, G3 50%W, and G3 75%W for the *in vivo* study. CBU_1910 has been used as an effective antigen of Q fever in previous studies ^{39,51} and was chosen as the antigen for the *in vivo* study. For controls, we also included PBS, pure CBU_1910 antigen protein, and alum in the study. Vaccines were prepared by mixing CBU 1910 antigen protein (3.3 µg) with PBS, alum (1 mg), or denpols (1 mg), respectively, and administered to mice intramuscularly on the hind legs on day 0 and day 14. The denpols were well tolerated in vivo as demonstrated by the weight growth curves (Figure S12). We used a protein microarray method to detect CBU 1910-specific total IgG, IgG1, and IgG2c in sera on day 28. Compared with CBU_1910 alone, alum and G3 50%W and G3 75%W helped generate significantly higher IgG signals (Figure 6A). The signals of IgG generated by them were similar. Regarding the subtype IgG1, both alum and denpols induced significantly stronger IgG1 signals than CBU_1910 alone and denpols with higher percentages of W were more active (Figure 6B). All experimental groups induced relatively low IgG2c signals, with both alum

and denpol adjuvants inducing some increase in the amount of IgG2c (Figure 6C). Notably, G3 75%W induced a significantly higher amount of IgG2c than CBU_1910 alone. Overall, the antibody results showed that the denpols, especially G3 50%W and G3 75%W, generated much higher total IgG signals than antigen alone, with stronger IgG1 signals compared to IgG2c. Since IgG1 is associated with Th2/humoral response and IgG2c is associated with Th1/cellular response 51, 52, both alum and denpols seemed to induce Th2-biased immune response, which was in agreement with previous studies of alum 34.

T cell responses are an indispensable part of antibody generation as CD4+ T cells induce specific B cells into plasma cells to generate antibodies. Therefore, we sacrificed mice on day 28 and studied the T cell responses by quantifying cytokines released into the supernatants from splenocytes cocultured with either CBU_1910 or an irrelevant antigen, OVA. Antigen-specific responses were observed for all immunized groups (Figure 6D and 6E). For Th2-associated cytokines (IL-5, IL-9, and IL-10) 53-55, CBU_1910 alone, alum, and denpol experimental groups all showed increased secretion upon the treatment of CBU_1910 (Figure 6E). Alum induced higher secretion of IL-5, IL-9, and IL-10 than denpols. For the alum group, the concentration of IL-5 was significantly higher than that of G3 25%W, and the concentration of IL-9 was significantly higher than those of G3 25%W and G3 75%W. In addition to generating Th2-associated cytokines, immunized groups also showed strong secretion of Th1-associated cytokines including IFN-y, TNF-α, and IL-2 (Figure 6D) ⁵⁶, which is consistent with detection of IgG2c in the serum. Among the denpol samples, G3 50%W consistently elicited the highest level of Th1-associated cytokines. G3 50%W induced a significantly higher amount of IFN-y than G3 25%W and both alum and G3 50%W helped secreted significantly higher amounts of TNF-α than G3 25%W. Notably, the IL-2 concentration in the G3 50%W group was more than 5-fold of that in the alum control group.

Similar to previous results that alum induced lower amounts of Th1-associated cytokines and higher amounts of Th2-associated cytokines compared with Th1-type adjuvants ¹⁸, alum and denpols in our study induced both Th1 and Th2-associated cytokines. Immunized groups also showed increased secretion of Th17-related cytokines including IL-17A, IL-17F, and IL-22 ⁵⁷, and the alum group had the highest amount of all cytokines (Figure S13). Neither alum nor denpols induced any antigen-specific CD8+ T cells in the spleen (Figure S14). Given the distinct cytokine profiles between alum and G3 50%W, even though they both presented Th2-biased responses based on the antibody result, they might induce intrinsically different T cell responses. Overall, the structure of G3 denpols also played a role in the *in vivo* antibody generation and T cell responses. Similar to the *in vitro* results, G3 50%W and G3 75%W were still the top performers *in vivo*.

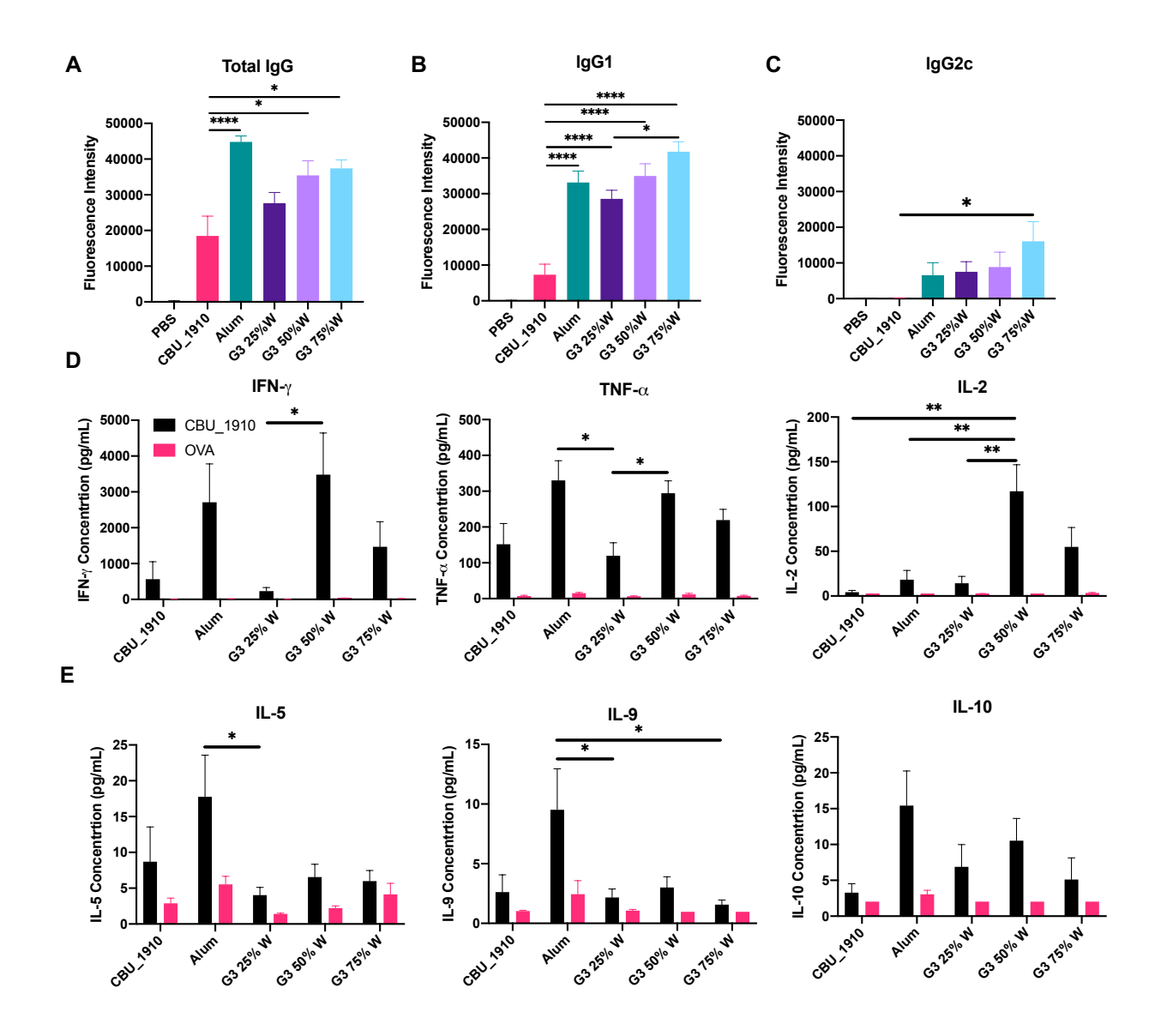


Figure 6. The adjuvanticity of denpols in *Coxiella burnetii* vaccines *in vivo*. A) Fluorescence intensities of CBU_1910 total IgG in sera collected on day 28. B) Fluorescence intensities of CBU_1910 IgG1 in sera collected on day 28. C) Fluorescence intensities of CBU_1910 IgG2c in sera collected on day 28. Mice were immunized with PBS, CBU_1910 (3.3 μ g), alum (1 mg) + CBU_1910 (3.3 μ g), G3 25%W (1 mg) + CBU_1910 (3.3 μ g), G3 50%W (1 mg) + CBU_1910 (3.3 μ g), or G3 75%W (1 mg) + CBU_1910 (3.3 μ g) on day 0 and day 14. The antibody intensities were measured using a protein microarray method. D) The concentrations of Th1-associated cytokines including IFN-γ, TNF-α, and IL-2 detected from the supernatants of splenocytes co-cultured with CBU_1910 (10 μ g/mL) or OVA (10 μ g/mL) for 16 h. E) The concentrations of Th2-associated cytokines including IL-5, IL-9, and IL-10 detected from the supernatants of splenocytes co-cultured with CBU_1910 (10 μ g/mL) or OVA (10 μ g/mL) for 16 h. Immunized mice were sacrificed on day 28 and splenocytes were isolated. Values are plotted as mean ± SEM (n = 5). For the statistical significance analysis, one-way ANOVA was employed with Tukey multiple

comparison test. *p < 0.05, **p < 0.01. For A and B, the statistical significance marked above columns were compared with the CBU_1910 group.

4. Conclusion

In summary, we prepared a series of G3 denpols with varying amounts of H and W functionalization to investigate the structure-activity correlation of their adjuvanticity for vaccine applications. G3 denpols demonstrated structure-dependent inflammasome activation in THP-1 cells and the activity increased with the percentages of W. By having different amounts of H and W, they also showed controlled BMDC activation and antigen cross-presentation. G3 50%W and G3 75%W increased the BMDC activation marker expression by more than 3-fold and antigen cross-presentation by more than 4-fold compared to traditional adjuvants such as LPS, CpG, MPLA, and alum. Flow cytometry and confocal microscopy data for cell uptake and distribution show that denpols with the optimal ratios of H/W (i.e, 50 and 75%W) exhibit both high cell uptake and sufficient endolysosomes rupture, which are in good agreement with the inflammasome activity in THP-1 cells and BMDC activation and antigen cross-presentation data. Finally, in vivo vaccination study using a Coxiella burnetii vaccine model showed that G3 denpols demonstrated structure-dependent adjuvanticity and generated significantly higher amount of antigen-specific antibodies than antigen alone. Denpols promoted a Th-2 biased antibody response but also induced Th1, Th2, and Th17 T cell responses. Taking together, both the *in vitro* and *in vivo* data show that G3 denpols exhibit relatively high and structure-dependent adjuvanticity. Given their easy and scalable synthesis, biodegradability, and tunable adjuvanticity, denpols are promising new adjuvants for vaccine applications. Their structural flexibility and high density of functional groups also allow for further structural permutations and conjugation of other adjuvating motifs to modulate or enhance their adjuvanticity.

Acknowledgements

This work was supported in part by the National Science Foundation grant DMR-2004555 (Guan, PI) and the Defense Threat Reduction Agency (DTRA) grant HDTRA1-18-1-0035 (Felgner, PI) and HDTRA-18-1-0036 (Davies, PI). The authors acknowledge the use of facilities and instrumentation at the UC Irvine Materials Research Institute (IMRI), which is supported in part by the National Science Foundation through the UC Irvine Materials Research Science and Engineering Center (DMR-2011967). This study was made possible in part through access to the Optical Biology Core Facility of the Developmental Biology Center, a shared resource supported by the Cancer Center Support Grant (CA-62203) and Center for Complex Biological Systems Support Grant (GM-076516) at the University of California, Irvine. The authors also thank Anna Gonzalez Rosell and Dr. Stacy M. Copp for assisting the Tecan measurement and Laser Spectroscopy Labs for the help with size and zeta-potential measurements.

Supplementing Information

The supporting Information is available free of charge at https://pubs.acs.org/doi/ Synthesis and characterization of denpols including 1H NMR spectra. In vitro and in vivo flow cytometry plots and other in vivo results.

References

- 1. Saxena, M.; van der Burg, S. H.; Melief, C. J. M.; Bhardwaj, N., Therapeutic cancer vaccines. *Nat Rev Cancer* **2021**, 21, 360-378.
- 2. Corbett, K. S.; Edwards, D. K.; Leist, S. R.; Abiona, O. M.; Boyoglu-Barnum, S.; Gillespie, R. A.; Himansu, S.; Schäfer, A.; Ziwawo, C. T.; DiPiazza, A. T.; Dinnon, K. H.; Elbashir, S. M.; Shaw, C. A.; Woods, A.; Fritch, E. J.; Martinez, D. R.; Bock, K. W.; Minai, M.; Nagata, B. M.; Hutchinson, G. B.; Wu, K.; Henry, C.; Bahl, K.; Garcia-Dominguez, D.; Ma, L.; Renzi, I.; Kong, W.-P.; Schmidt, S. D.;

- Wang, L.; Zhang, Y.; Phung, E.; Chang, L. A.; Loomis, R. J.; Altaras, N. E.; Narayanan, E.; Metkar, M.; Presnyak, V.; Liu, C.; Louder, M. K.; Shi, W.; Leung, K.; Yang, E. S.; West, A.; Gully, K. L.; Stevens, L. J.; Wang, N.; Wrapp, D.; Doria-Rose, N. A.; Stewart-Jones, G.; Bennett, H.; Alvarado, G. S.; Nason, M. C.; Ruckwardt, T. J.; McLellan, J. S.; Denison, M. R.; Chappell, J. D.; Moore, I. N.; Morabito, K. M.; Mascola, J. R.; Baric, R. S.; Carfi, A.; Graham, B. S., SARS-CoV-2 mRNA vaccine design enabled by prototype pathogen preparedness. *Nature* **2020**, 586, 567-571.
- 3. Wang, Z.; Schmidt, F.; Weisblum, Y.; Muecksch, F.; Barnes, C. O.; Finkin, S.; Schaefer-Babajew, D.; Cipolla, M.; Gaebler, C.; Lieberman, J. A.; Oliveira, T. Y.; Yang, Z.; Abernathy, M. E.; Huey-Tubman, K. E.; Hurley, A.; Turroja, M.; West, K. A.; Gordon, K.; Millard, K. G.; Ramos, V.; Da Silva, J.; Xu, J.; Colbert, R. A.; Patel, R.; Dizon, J.; Unson-O'Brien, C.; Shimeliovich, I.; Gazumyan, A.; Caskey, M.; Bjorkman, P. J.; Casellas, R.; Hatziioannou, T.; Bieniasz, P. D.; Nussenzweig, M. C., mRNA vaccine-elicited antibodies to SARS-CoV-2 and circulating variants. *Nature* **2021**, 592, 616-622.
- 4. Mulligan, M. J.; Lyke, K. E.; Kitchin, N.; Absalon, J.; Gurtman, A.; Lockhart, S.; Neuzil, K.; Raabe, V.; Bailey, R.; Swanson, K. A.; Li, P.; Koury, K.; Kalina, W.; Cooper, D.; Fontes-Garfias, C.; Shi, P.-Y.; Türeci, Ö.; Tompkins, K. R.; Walsh, E. E.; Frenck, R.; Falsey, A. R.; Dormitzer, P. R.; Gruber, W. C.; Şahin, U.; Jansen, K. U., Phase I/II study of COVID-19 RNA vaccine BNT162b1 in adults. *Nature* **2020**, 586, 589-593.
- 5. Li, J.; Hui, A.; Zhang, X.; Yang, Y.; Tang, R.; Ye, H.; Ji, R.; Lin, M.; Zhu, Z.; Türeci, Ö.; Lagkadinou, E.; Jia, S.; Pan, H.; Peng, F.; Ma, Z.; Wu, Z.; Guo, X.; Shi, Y.; Muik, A.; Şahin, U.; Zhu, L.; Zhu, F., Safety and immunogenicity of the SARS-CoV-2 BNT162b1 mRNA vaccine in younger and older Chinese adults: a randomized, placebo-controlled, double-blind phase 1 study. *Nat. Med.* **2021**, 27, 1062-1070.
- 6. Assis, R.; Jain, A.; Nakajima, R.; Jasinskas, A.; Kahn, S.; Palma, A.; Parker, D. M.; Chau, A.; Leung, A.; Grabar, C.; Muqolli, F.; Khalil, G.; Escobar, J. C.; Ventura, J.; Davies, D. H.; Albala, B.; Boden-Albala, B.; Schubl, S.; Felgner, P. L., Substantial Differences in SARS-CoV-2 Antibody Responses Elicited by Natural Infection and mRNA Vaccination. *bioRxiv* **2021**, 2021.04.15.440089.
- 7. Han, S., Clinical vaccine development. *Clin Exp Vaccine Res* **2015**, 4, 46-53.
- 8. Kranz, L. M.; Diken, M.; Haas, H.; Kreiter, S.; Loquai, C.; Reuter, K. C.; Meng, M.; Fritz, D.; Vascotto, F.; Hefesha, H.; Grunwitz, C.; Vormehr, M.; Hüsemann, Y.; Selmi, A.; Kuhn, A. N.; Buck, J.; Derhovanessian, E.; Rae, R.; Attig, S.; Diekmann, J.; Jabulowsky, R. A.; Heesch, S.; Hassel, J.; Langguth, P.; Grabbe, S.; Huber, C.; Türeci, Ö.; Sahin, U., Systemic RNA delivery to dendritic cells exploits antiviral defence for cancer immunotherapy. *Nature* **2016**, 534, 396-401.
- 9. Yadav, M.; Jhunjhunwala, S.; Phung, Q. T.; Lupardus, P.; Tanguay, J.; Bumbaca, S.; Franci, C.; Cheung, T. K.; Fritsche, J.; Weinschenk, T.; Modrusan, Z.; Mellman, I.; Lill, J. R.; Delamarre, L., Predicting immunogenic tumour mutations by combining mass spectrometry and exome sequencing. *Nature* **2014**, 515, 572-576.
- 10. Jansen, K. U.; Girgenti, D. Q.; Scully, I. L.; Anderson, A. S., Vaccine review: "Staphyloccocus aureus vaccines: Problems and prospects". *Vaccine* **2013**, 31, 2723-2730.
- 11. Girard, M. P.; Cherian, T.; Pervikov, Y.; Kieny, M. P., A review of vaccine research and development: Human acute respiratory infections. *Vaccine* **2005**, 23, 5708-5724.
- 12. Moyer, T. J.; Kato, Y.; Abraham, W.; Chang, J. Y. H.; Kulp, D. W.; Watson, N.; Turner, H. L.; Menis, S.; Abbott, R. K.; Bhiman, J. N.; Melo, M. B.; Simon, H. A.; Herrera-De la Mata, S.; Liang, S.; Seumois, G.; Agarwal, Y.; Li, N.; Burton, D. R.; Ward, A. B.; Schief, W. R.; Crotty, S.; Irvine, D. J.,

- Engineered immunogen binding to alum adjuvant enhances humoral immunity. *Nat. Med.* **2020,** 26, 430-440.
- 13. Capietto, A.-H.; Jhunjhunwala, S.; Pollock, S. B.; Lupardus, P.; Wong, J.; Hänsch, L.; Cevallos, J.; Chestnut, Y.; Fernandez, A.; Lounsbury, N.; Nozawa, T.; Singh, M.; Fan, Z.; de la Cruz, C. C.; Phung, Q. T.; Taraborrelli, L.; Haley, B.; Lill, J. R.; Mellman, I.; Bourgon, R.; Delamarre, L., Mutation position is an important determinant for predicting cancer neoantigens. *J. Exp. Med.* **2020**, 217, e20190179.
- 14. Sahin, U.; Muik, A.; Derhovanessian, E.; Vogler, I.; Kranz, L. M.; Vormehr, M.; Baum, A.; Pascal, K.; Quandt, J.; Maurus, D.; Brachtendorf, S.; Lörks, V.; Sikorski, J.; Hilker, R.; Becker, D.; Eller, A.-K.; Grützner, J.; Boesler, C.; Rosenbaum, C.; Kühnle, M.-C.; Luxemburger, U.; Kemmer-Brück, A.; Langer, D.; Bexon, M.; Bolte, S.; Karikó, K.; Palanche, T.; Fischer, B.; Schultz, A.; Shi, P.-Y.; Fontes-Garfias, C.; Perez, J. L.; Swanson, K. A.; Loschko, J.; Scully, I. L.; Cutler, M.; Kalina, W.; Kyratsous, C. A.; Cooper, D.; Dormitzer, P. R.; Jansen, K. U.; Türeci, Ö., COVID-19 vaccine BNT162b1 elicits human antibody and TH1 T cell responses. *Nature* **2020**, 586, 594-599.
- 15. Pulendran, B.; S. Arunachalam, P.; O'Hagan, D. T., Emerging concepts in the science of vaccine adjuvants. *Nat. Rev. Drug Discov.* **2021**, 20, 454-475.
- 16. Awate, S.; Babiuk, L. A.; Mutwiri, G., Mechanisms of action of adjuvants. *Front Immunol* **2013**, 4, 114-114.
- 17. Marshall, J. S.; Warrington, R.; Watson, W.; Kim, H. L., An introduction to immunology and immunopathology. *Allergy Asthma Clin. Immunol.* **2018,** 14, 49.
- 18. Korsholm, K. S.; Petersen, R. V.; Agger, E. M.; Andersen, P., T-helper 1 and T-helper 2 adjuvants induce distinct differences in the magnitude, quality and kinetics of the early inflammatory response at the site of injection. *Immunology* **2010**, 129, 75-86.
- 19. Shi, S.; Zhu, H.; Xia, X.; Liang, Z.; Ma, X.; Sun, B., Vaccine adjuvants: Understanding the structure and mechanism of adjuvanticity. *Vaccine* **2019**, 37, 3167-3178.
- 20. Gavin, A. L.; Hoebe, K.; Duong, B.; Ota, T.; Martin, C.; Beutler, B.; Nemazee, D., Adjuvant-enhanced antibody responses in the absence of toll-like receptor signaling. *Science* **2006**, 314, 1936-1938.
- 21. Marrack, P.; McKee, A. S.; Munks, M. W., Towards an understanding of the adjuvant action of aluminium. *Nat. Rev. Immunol.* **2009,** 9, 287-293.
- 22. Ellebedy, A. H.; Lupfer, C.; Ghoneim, H. E.; DeBeauchamp, J.; Kanneganti, T.-D.; Webby, R. J., Inflammasome-independent role of the apoptosis-associated speck-like protein containing CARD (ASC) in the adjuvant effect of MF59. *Proc. Natl. Acad. Sci. U.S.A.* **2011**, 108, 2927-2932.
- 23. Morel, S.; Didierlaurent, A.; Bourguignon, P.; Delhaye, S.; Baras, B.; Jacob, V.; Planty, C.; Elouahabi, A.; Harvengt, P.; Carlsen, H.; Kielland, A.; Chomez, P.; Garçon, N.; Van Mechelen, M., Adjuvant System ASO3 containing α -tocopherol modulates innate immune response and leads to improved adaptive immunity. *Vaccine* **2011**, 29, 2461-2473.
- 24. Garçon, N.; Di Pasquale, A., From discovery to licensure, the Adjuvant System story. *Hum. Vaccines Immunother.* **2017**, 13, 19-33.
- 25. Lee, G. H.; Lim, S. G., CpG-Adjuvanted Hepatitis B Vaccine (HEPLISAV-B®) Update. *Expert Rev Vaccines* **2021**, 20, 487-495.
- 26. Kensil, C. R., Saponins as vaccine adjuvants. Crit Rev Ther Drug Carrier Syst 1996, 13, 1-55.
- 27. Welsby, I.; Detienne, S.; N'Kuli, F.; Thomas, S.; Wouters, S.; Bechtold, V.; De Wit, D.; Gineste, R.; Reinheckel, T.; Elouahabi, A.; Courtoy, P. J.; Didierlaurent, A. M.; Goriely, S.,

- Lysosome-Dependent Activation of Human Dendritic Cells by the Vaccine Adjuvant QS-21. *Front Immunol* **2016,** 7, 663.
- 28. Gallorini, S.; Berti, F.; Parente, P.; Baronio, R.; Aprea, S.; D'Oro, U.; Pizza, M.; Telford, J. L.; Wack, A., Introduction of Zwitterionic Motifs into Bacterial Polysaccharides Generates TLR2 Agonists Able to Activate APCs. *J. Immunol.* **2007**, 179, 8208-8215.
- 29. Laurent, X.; Bertin, B.; Renault, N.; Farce, A.; Speca, S.; Milhomme, O.; Millet, R.; Desreumaux, P.; Hénon, E.; Chavatte, P., Switching invariant natural killer T (iNKT) cell response from anticancerous to anti-inflammatory effect: molecular bases. *J. Med. Chem.* **2014,** 57, 5489-508.
- 30. Stoker, K.; Levien, T. L.; Baker, D. E., Zoster Vaccine Recombinant, Adjuvanted. *Hosp Pharm* **2018**, 53, 136-141.
- 31. Shakya, A. K.; Nandakumar, K. S., Applications of polymeric adjuvants in studying autoimmune responses and vaccination against infectious diseases. *J. R. Soc. Interface* **2013**, 10, 20120536.
- 32. Luo, M.; Wang, H.; Wang, Z.; Cai, H.; Lu, Z.; Li, Y.; Du, M.; Huang, G.; Wang, C.; Chen, X.; Porembka, M. R.; Lea, J.; Frankel, A. E.; Fu, Y.-X.; Chen, Z. J.; Gao, J., A STING-activating nanovaccine for cancer immunotherapy. *Nat. Nanotechnol.* **2017**, 12, 648-654.
- 33. Xu, J.; Lv, J.; Zhuang, Q.; Yang, Z.; Cao, Z.; Xu, L.; Pei, P.; Wang, C.; Wu, H.; Dong, Z.; Chao, Y.; Wang, C.; Yang, K.; Peng, R.; Cheng, Y.; Liu, Z., A general strategy towards personalized nanovaccines based on fluoropolymers for post-surgical cancer immunotherapy. *Nat. Nanotechnol.* **2020**, 15, 1043-1052.
- 34. Steinbuck, M. P.; Seenappa, L. M.; Jakubowski, A.; McNeil, L. K.; Haqq, C. M.; DeMuth, P. C., A lymph node—targeted Amphiphile vaccine induces potent cellular and humoral immunity to SARS-CoV-2. *Sci. Adv.* **2021,** 7, eabe5819.
- 35. Sun, B.; Ji, Z.; Liao, Y. P.; Wang, M.; Wang, X.; Dong, J.; Chang, C. H.; Li, R.; Zhang, H.; Nel, A. E.; Xia, T., Engineering an effective immune adjuvant by designed control of shape and crystallinity of aluminum oxyhydroxide nanoparticles. *ACS Nano* **2013**, 7, 10834-49.
- 36. Zeng, H.; Little, H. C.; Tiambeng, T. N.; Williams, G. A.; Guan, Z., Multifunctional Dendronized Peptide Polymer Platform for Safe and Effective siRNA Delivery. *J. Am. Chem. Soc.* **2013**, 135, 4962-4965.
- 37. Oldenhuis, N. J.; Eldredge, A. C.; Burts, A. O.; Ryu, K. A.; Chung, J.; Johnson, M. E.; Guan, Z., Biodegradable Dendronized Polymers for Efficient mRNA Delivery. *ChemistrySelect* **2016**, 1, 4413-4417.
- 38. Manna, S.; Howitz, W. J.; Oldenhuis, N. J.; Eldredge, A. C.; Shen, J.; Nihesh, F. N.; Lodoen, M. B.; Guan, Z.; Esser-Kahn, A. P., Immunomodulation of the NLRP3 Inflammasome through Structure-Based Activator Design and Functional Regulation via Lysosomal Rupture. *ACS Cent. Sci.* **2018**, *4*, 982-995.
- 39. Fratzke, A. P.; Jan, S.; Felgner, J.; Liang, L.; Nakajima, R.; Jasinskas, A.; Manna, S.; Nihesh, F. N.; Maiti, S.; Albin, T. J.; Esser-Kahn, A. P.; Davies, D. H.; Samuel, J. E.; Felgner, P. L.; Gregory, A. E., Subunit Vaccines Using TLR Triagonist Combination Adjuvants Provide Protection Against Coxiella burnetii While Minimizing Reactogenic Responses. *Front Immunol* **2021**, 12, 790.
- 40. Metzke, M.; O'Connor, N.; Maiti, S.; Nelson, E.; Guan, Z., Saccharide-peptide hybrid copolymers as biomaterials. *Angew. Chem. Int. Ed.* **2005**, 44, 6529-33.

- 41. Chanput, W.; Mes, J.; Vreeburg, R. A.; Savelkoul, H. F.; Wichers, H. J., Transcription profiles of LPS-stimulated THP-1 monocytes and macrophages: a tool to study inflammation modulating effects of food-derived compounds. *Food Funct* **2010**, 1, 254-61.
- 42. Sun, B.; Ji, Z.; Liao, Y.-P.; Chang, C. H.; Wang, X.; Ku, J.; Xue, C.; Mirshafiee, V.; Xia, T., Enhanced Immune Adjuvant Activity of Aluminum Oxyhydroxide Nanorods through Cationic Surface Functionalization. *ACS Applied Materials & Interfaces* **2017**, 9, 21697-21705.
- 43. Linsley, P. S.; Greene, J. L.; Brady, W.; Bajorath, J.; Ledbetter, J. A.; Peach, R., Human B7-1 (CD80) and B7-2 (CD86) bind with similar avidities but distinct kinetics to CD28 and CTLA-4 receptors. *Immunity* **1994**, 1, 793-801.
- 44. Kuai, R.; Ochyl, L. J.; Bahjat, K. S.; Schwendeman, A.; Moon, J. J., Designer vaccine nanodiscs for personalized cancer immunotherapy. *Nat. Mater.* **2017**, 16, 489-496.
- 45. Ma, D. Y.; Clark, E. A., The role of CD40 and CD154/CD40L in dendritic cells. *Semin. Immunol.* **2009**, 21, 265-272.
- 46. Roche, P. A.; Furuta, K., The ins and outs of MHC class II-mediated antigen processing and presentation. *Nat. Rev. Immunol.* **2015**, 15, 203-216.
- 47. Rydberg, H. A.; Matson, M.; Åmand, H. L.; Esbjörner, E. K.; Nordén, B., Effects of Tryptophan Content and Backbone Spacing on the Uptake Efficiency of Cell-Penetrating Peptides. *Biochemistry* **2012**, 51, 5531-5539.
- 48. Wen, Y.; Guo, Z.; Du, Z.; Fang, R.; Wu, H.; Zeng, X.; Wang, C.; Feng, M.; Pan, S., Serum tolerance and endosomal escape capacity of histidine-modified pDNA-loaded complexes based on polyamidoamine dendrimer derivatives. *Biomaterials* **2012**, 33, 8111-21.
- 49. Sonawane, N. D.; Szoka, F. C.; Verkman, A. S., Chloride Accumulation and Swelling in Endosomes Enhances DNA Transfer by Polyamine-DNA Polyplexes*. *J. Biol. Chem.* **2003**, 278, 44826-44831.
- 50. Wang, X.; Chang, C. H.; Jiang, J.; Liu, Q.; Liao, Y.-P.; Lu, J.; Li, L.; Liu, X.; Kim, J.; Ahmed, A.; Nel, A. E.; Xia, T., The Crystallinity and Aspect Ratio of Cellulose Nanomaterials Determine Their Pro-Inflammatory and Immune Adjuvant Effects In Vitro and In Vivo. *Small* **2019**, 15, 1901642.
- 51. Gilkes, A. P.; Albin, T. J.; Manna, S.; Supnet, M.; Ruiz, S.; Tom, J.; Badten, A. J.; Jain, A.; Nakajima, R.; Felgner, J.; Davies, D. H.; Stetkevich, S. A.; Zlotnik, A.; Pearlman, E.; Nalca, A.; Felgner, P. L.; Esser-Kahn, A. P.; Burkhardt, A. M., Tuning Subunit Vaccines with Novel TLR Triagonist Adjuvants to Generate Protective Immune Responses against Coxiella burnetii. *J. Immunol.* **2020**, 204, 611-621.
- 52. Mosmann, T. R.; Coffman, R. L., Two types of mouse helper T-cell clone Implications for immune regulation. *Immunol. Today* **1987**, 8, 223-7.
- 53. Zhou, Y.; McLane, M.; Levitt, R. C., Th2 cytokines and asthma. Interleukin-9 as a therapeutic target for asthma. *Respir. Res.* **2001,** 2, 80-84.
- 54. Torre, D.; Speranza, F.; Giola, M.; Matteelli, A.; Tambini, R.; Biondi, G., Role of Th1 and Th2 Cytokines in Immune Response to Uncomplicated Plasmodium falciparum Malaria. *Clin. Diagn. Lab. Immunol.* **2002,** 9, 348-351.
- 55. Lambrecht, B. N.; Hammad, H.; Fahy, J. V., The Cytokines of Asthma. *Immunity* **2019**, 50, 975-991.
- 56. Seder, R. A.; Darrah, P. A.; Roederer, M., T-cell quality in memory and protection: implications for vaccine design. *Nat Rev Immunol* **2008**, 8, 247-58.

57. Guglani, L.; Khader, S. A., Th17 cytokines in mucosal immunity and inflammation. *Curr Opin HIV AIDS* **2010**, 5, 120-127.

For Table of Contents Only

